A Positioning Alarm System for Explosive Impact Debris Protective Suit Based on Accelerometer Array

Jianing Hu , Chaoran Liu * , Xucong Wang , Zai Wang , Xin Tong , Fangqi Li , Zhenyu Jin , Xiaoyuan Wang , Lufeng Che , Jing Yu , Defei Yao , Gaofeng Wang , Linxi Dong

Posted Date: 6 June 2024

doi: 10.20944/preprints202406.0345.v1

Keywords: Protection suit; debris positioning alarm system; accelerometer array; real-time monitoring

Article

A Positioning Alarm System for Explosive Impact Debris Protective Suit Based on Accelerometer Array

Jianing Hu [1], Chaoran Liu [1,*], Xucong Wang [1], Zai Wang [1], Xin Tong [1], Fangqi Li [1], Zhenyu Jin [1], Xiaoyuan Wang [2], Lufeng Che [3], Jing Yu [2], Defei Yao [2,*], Gaofeng Wang [1] and Linxi Dong [1,*]

[1] Ministry of Education Engineering Research Center of Smart Microsensors and Microsystems, College of Electronics and Information, Hangzhou Dianzi University, Hangzhou 310018, People's Republic of China
[2] Zhejiang KeyLaboratory ofEcological and Environmental Big Data, Hangzhou, 321001, People's Republic of China
[3] College of Information Science and Electronic Engineering, Zhejiang University, Hangzhou 310027, People's Republic of China
* Correspondence: liucr@hdu.edu.cn, 38151298@qq.com and donglinxi@hdu.edu.cn

Abstract: Protection suit is vital for fireman' safety. Traditional protection suit just physically protects fireman from empyrosis, but can not locate the body injury position from the impact debris. Herein, we present a wearable impact debris positioning system for fireman protection suit alarming based on accelerometer array. The wearable piezoelectric accelerometers with distribute regularly on the suit to detect the vibration on different body parts, which is conducive to positioning injured body parts. In addition, the injured parts can be displayed on the dummy body model on the upper computer with a higher localization accuracy of 4 cm. The positioning alarm system has a rapid response time of 0.11ms attributing to smart signal processing method. This work provides a reliable and smart method for locating and assessing the body injury position from the impact debris, which is significant for fire disaster commander to rescue injured fireman in time.

Keywords: protection suit; debris positioning alarm system; accelerometer array; real-time monitoring

1. Introduction

In the fire rescue work, the personal safety of firefighters has always been the focus of public concern[1].The fire scene environment is harsh, volatile, complex terrain and poor visual conditions[2]. Smart protection suits embedding sensor array are conducive to fill the gap of traditional camera vision and to detect the fireman injuries and personal safety[3]. Developing wearable protection suit with smart safety detection system has great significance to real-time monitor fireman injure condition and the explosive debris impacted on body parts, which is a significant subject.

Elegant approaches have explored to develop smart protection suits for fireman. More and more highly sensitivity and reliable sensors are applied to the suits to monitor more safety information about rescuing fireman. Attributing to the higher sensitive to hyperthermia[4,5], carbon nanotube has been applied for high-temperature sensor and warning of protection suits to avoid fireman empyrosis[6]. In addition, IoT sensors[7,8] combining with dynamic sensing and GPS technology achieve the precising positioning of fireman for timely medical treatment[9,10]. Moreover, wearable sensors for detecting human physiological parameters such as blood oxygen concentration, pulse, respiratory et al[9,11], have been applied on protection suits for fireman[9,12].

Herein, we present a positioning alarm system for explosive impact debris protective suit based on accelerometer array. Our suit system achieves the locating the body injury position from the impact debris, which is superior to the traditional protection suit without quantitative analysis and position of injuries, our suit system achieves the locating the body injury position from the impact debris. The piezoelectric acceleration sensors array on different body parts, achieving the real-time detection of injuring and impact on different body position. Moreover, human vitals such as heart has more denser accelerometers to monitor precisely. For the signal circuit system, we employ the

 doi:10.20944/preprints202406.0345.v1

UART-DMA to accelerate the data processing, which shortens the per data processing period to 110 μs. This developed protection suit with explosive impact debris positioning alarm system can real-time monitoring and assessing the body injury position of fireman.

2. System Design

We develop a smart protection suit system integrated with high-sensitivity piezoelectric patch accelerometer array to monitor the safety of fireman operating in hazardous situation. These sensors are install in body vital parts[13] such as the heart, back and limbs as shown in Figure 1. As the explosive debris impact on fireman, the suit system can detect the impact body position and intensity by the arrayed sensor enabled by the piezoelectric effect, accordingly assessing the severity of injury. The novel designed suit system can real-time monitor the intensity of impact force and precisely locate the injure on fireman body in complex dynamic situation simultaneously.

The acceleration sensors detect the impact[14,15] and submit the signal to an embedded microcontroller system though a high-performance analog-to-digital converter (ADC) transforms[16]. The microcontroller system enables wireless transmission the processed signal to an upper computer system in serial communication via an integrated Bluetooth module. After that, the upper computer decodes and parses the serial data, evaluating the harm inflicted on human body. The analyses are visualized on a realistic 3D human model, which enables monitoring personnel to identify the impacted areas. Thus, rescue and protective strategies can be facilitated immediately. The system provides revolutionary technical support and assurance for personnel safety in high-risk environments.

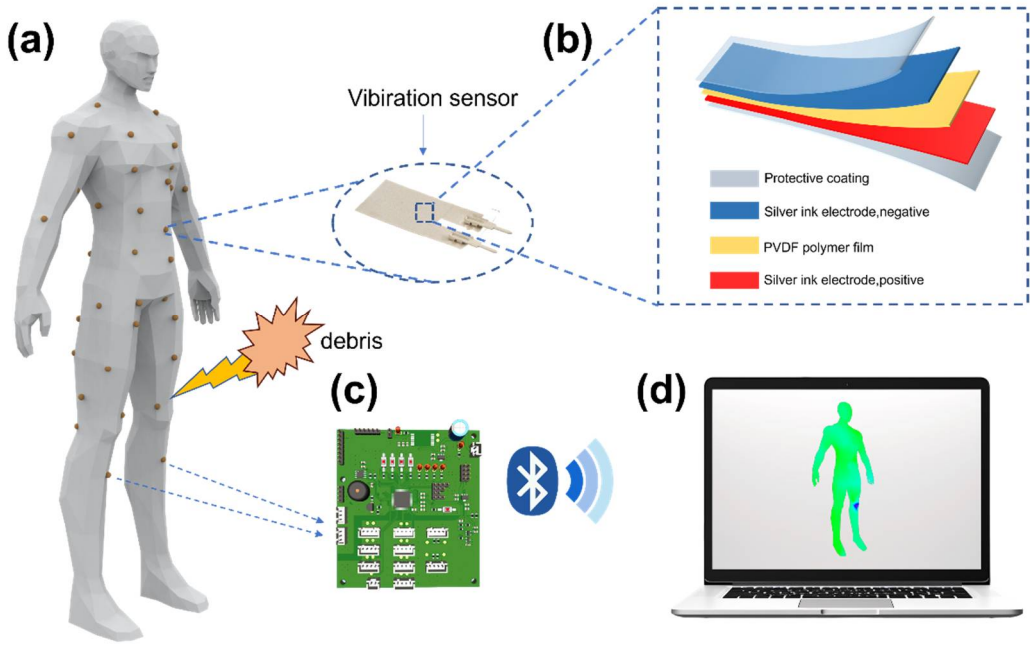

Figure 1. Constitution of the position alarm system. (a) Mannequin with sensors distributed. (b) Structure of the piezoelectric sensor. (c) Single-chip system. (d) Host system.

2.1. Piezoelectric Sensor Selection and Structural Analysis

Sensor performance is critical to system, as it is the foremost part of signal acquisition. Acceleration sensors are employed to capture impact signals from external flying debris.

Piezoelectric sensor is fabricated based on the piezoelectric effect[17], which has the advantages of high sensitivity, a high signal-to-noise ratio, simple structure, compact size, light weight, low power consumption, long lifespan, and reliable operation. With the excellent dynamic characteristics, it enables detecting periodic forces with wide frequency bands and rapid changes caused by impact forces.

The selected sensor consists of 5 layers, including two protective coating layers, two silver ink electrodes, and PVDF (polyvinylidene fluoride) polymer film as shown in Figure 1. When compressing the PVDF polymer film, positive and negative charges are induced on its surface.

 doi:10.20944/preprints202406.0345.v1

Through highly conductive silver ink electrodes[18], the charges are transmitted to the charge amplifiers for analysis.

2.2. Hardware Circuit

The induced charge from piezoelectric film is too weak for a microcontroller system, necessitating signal amplification through a front-end amplifier[19].

Firstly, designing a voltage amplifier when the sensor is treated as an equivalent voltage source[20]. The analysis indicates that the minuscule charge induced by the sensor leaks through its internal resistance (Ra) and the input resistance of amplifier (Ri), hindering the measurement of static mechanical quantities. Additionally, the sensor sensitivity is related to the input capacitance (comprising sensor capacitance Ca, amplifier input capacitance Ci, and lead capacitance Cc). Thus, the sensitivity requires recalculation when altering the wire length, complicating the design process.

Then, designing a charge amplifier when the sensor is treated as an equivalent charge source. This type of amplifier can ignore the influence from input and cable capacitances to the output voltage, whose voltage only depends on the charge input and the feedback capacitance[21,22]. The effects from wire length are eliminated.

Hence, charge amplifiers are chosen as the measurement circuit for the piezoelectric sensors. The charge amplifier is a high-gain amplifier with deep negative feedback[23]. The low bias current for minimal charge loss, low offset for accuracy, low-voltage operation to minimize power consumption, and high precision are considered in the selection of amplifier chip, which decreases the charge loss and power dissipation[24].

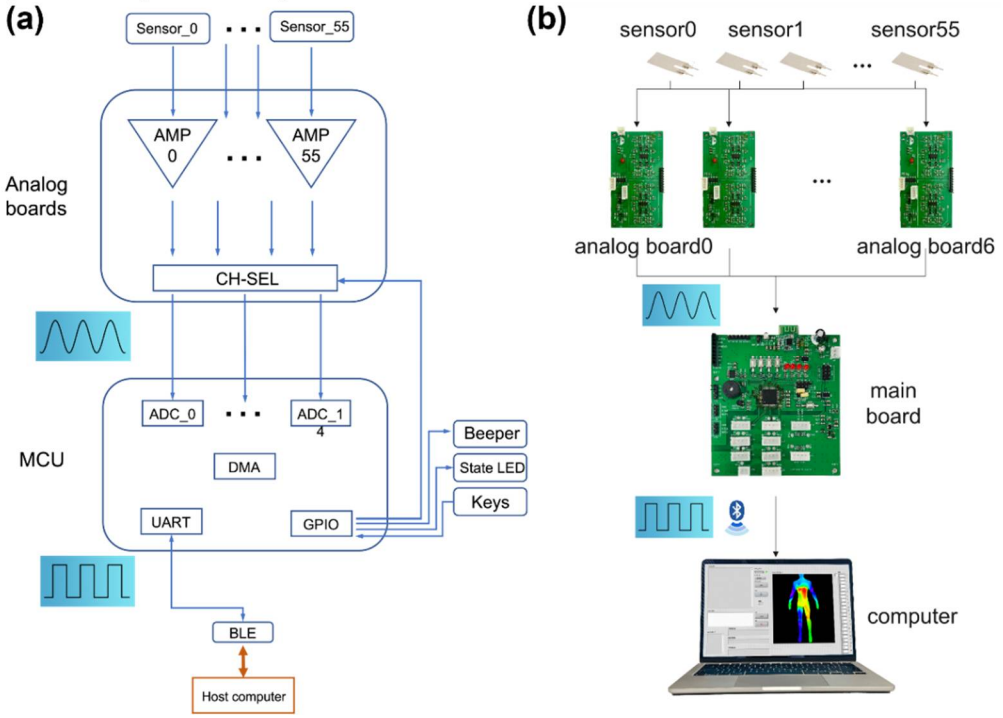

Figure 2. The process of how the system works. (a)Schematic diagram. (b)Real products.

The GS8334 chip is adopted as the core component for the charge amplifier. At the input stage, a 50 Hz dual-T notch filter is utilized to mitigate the industrial frequency interference. Additionally, a first-order RC high-pass filter is included to remove DC signals; a pair of back-to-back diodes are placed in parallel to protect the operational amplifier from overvoltage. Since the structure of charge amplifier is similar to integrator circuit, a large resistor is paralleled across the feedback capacitor to prevent the output saturation. Here, the increased resistance value ensures an appropriate hold time for the output signal.

The microcontroller system is powered by a 5 V battery. An HT7333 LDO (Low Dropout) linear regulator is employed in the analog front-end to step down the 5 V input to 3.3 V. Without deformation on the piezoelectric film, the output of the charge amplifier is designed to 1.65 V, which ensures symmetrical detection of deformations in both directions. Therefore, a TL431 is precisely

 doi:10.20944/preprints202406.0345.v1

parallel connected to voltage regulator to generate a stable 2.5 V potential, with its reference terminal short to the cathode. After voltage is divided to 1.65 V, it is transmitted to a high-input impedance voltage follower for buffering, resulting in a stable 1.65 V supply for the positive input of the charge amplifier.

To accommodate the limited ADC channels on the MCU, a CH444 dual SP4T (Double pole four throw) analog switch IC is employed. It transmits the processed signal from analog front end panel in phases to MCU, dividing a full cycle into four stages, with each stage transmitting data from two channels.

The microcontroller system needs to complete the ADC signal acquisition, encoding and transmitting to serial port. Hence, more ADC channels are required to increase ADC conversion precision and faster operation rate. Balancing cost-effectiveness with performance, the STC8H8K64U (based on the 8051 core) is chosen for this application. It operates at a maximum clock frequency of 45MHz and is equipped with DMA (Direct Memory Access) capabilities, enhancing data transfer efficiency. Besides, this MCU has a 12-bit ADC with 15 channels, capable of achieving a maximum sampling rate of approximately 800 KS/s.

The HT7333 module is utilized to power the system, converting the standard 5 V input voltage to the 3.3 V required by the MCU. It is a versatile LDO (low dropout regulator) known for its excellent performance with among 300mA output current, with minimal standby current of just 2 μA and an output voltage accuracy within ±2%. Capacitors are placed at both the input and output sides of the HT7333 to filter the power ripple.

An onboard Bluetooth module is incorporated to enable the wireless transmission. Considering the relatively high power-consumption of Bluetooth transmission, a separate HT7333 is dedicated to powering the Bluetooth module. The RXD and TXD pins of the Bluetooth module are connected to the TxD3 and RxD3 pins of the MCU respectively, facilitating serial communication.

The A/D conversion requires a precise 3.3 V reference voltage. A TL431 precision shunt regulator is employed to generate a stable 2.5V, which is then buffered by a voltage follower to produce a 3.3V reference voltage. Consequently, it is connected to the MCU's ADC reference voltage pin.

Furthermore, a beeper is added to the board to alarm, with an S8050 transistor amplifies the current from the MCU. Four buttons and four LEDs are integrated into the design, instructing the circuit's operation. An EEPROM is included communicating with the MCU through the I^2C protocol, which allows for post-mission review of the protective suit's impact.

2.3. Software Program

The framework is established by configuring timers (generate specific baud rate) and registers related to ADC and UART. The ADC and UART are hindered by waiting for register access when the data is transmitted by UART and ADC respectively. Hence, to improve the data moving efficiency, two buffer arrays are established to hold the data temporarily and global interrupts are turned on. Consequently, DMA (direct memory access) is configured for the ADC to automatically move sensor data from the ADC registers to Buffer Array 1, which enables the CPU to deal with other tasks. Upon the data transfer is completed, the contents of Buffer Array 1 are copied to Buffer Array 2, and DMA starts the next data acquisition cycle immediately. Meanwhile, the DMA of UART is configured to transfer data from Buffer Array 2 to the UART interface, freeing the CPU either.

Although the MCU offers a 12-bit resolution ADC, the high precision makes no difference in the fragment impact analysis, which wastes the resources of upper computer and serial ports. Therefore, the first three bits of each sensor's data are retained, which are converted to hexadecimal and then packed in to Buffer Array 2. Besides, a frame end identifier is appended to the end of each data packet in Buffer Array 2 to demarcate individual data frames. To reduce the process period, the MCU's internal clock speed is increased to 33.1776 MHz, and the UART baud rate is escalated to 921,600 bits per second. After processing, the encoded data is wirelessly transmitted to the upper computer through the Bluetooth module.

 doi:10.20944/preprints202406.0345.v1

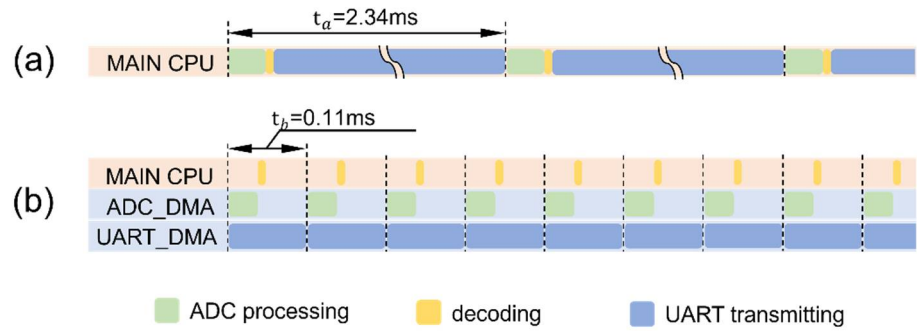

Figure 3. The comparison of the system cycle.(a)the cycle of system without DMA.(b)the cycle of system with DMA.

The upper computer employed LabVIEW (Laboratory Virtual instrument Engineering Workbench) software as the primary environment, which constitutes a graphical programming platform extensively acknowledged by the industrial sector, academia, and research institutions[25]. serves as a benchmark for applications involving data acquisition and instrument control. LabVIEW integrates comprehensive capabilities for communication with hardware conforming to protocols such as GPIB (General Purpose Interface Bus), VXI (VME Extensions for Instrumentation), RS-232, and RS-485, along with data acquisition cards. Moreover, it includes libraries that simplify adherence to software standards like TCP/IP and ActiveX, augmenting its versatility[26].

The project utilizes VISA controls to achieve serial communication functionalities, enabling sending and receiving of data[27,28]. By employing a "state machine" concept realized through Condition structures, different operational states of the host computer are simulated. Moreover, buttons, string indicators, and input controls are included to facilitate selection of serial baud rates and enable free data transmission and reception.

2.4. State Machine Partitioning

A state machine[29] is a mathematical model to describe the logical behavior of a control system. It represents a finite number of states, the transitions between them, and the conditions for these transitions. Here, we adopted a Moore state machine, where the output depends not only on the current state, but also on the input that triggered the transition[30]. The states are as follows:

2.4.1. Init State

It is the initial system state where all arrays are reset to zero, and the serial port baud rate is set to 921,600 before transitioning to the Wait state.

2.4.2. Wait State

If the serial port is closed, the system remains in this loop. Upon opening the serial port, it transitions to the GetData state. While in this state, it responds to button events:

- Serial_Open Button: If the port is closed, sets the port name and baud rate, opens the port, and moves to GetData state. If open, closes the port and stays in Wait.
- Clear Button: Resets all arrays to zero. If the port is open, proceeds to GetData; if closed, remains in Wait.
- Exit Button: Transitions to Exit state, closing the serial port and terminating the LabVIEW program if open, or exits directly if the port is already closed.

2.4.3. GetData State

Upon receiving data through the serial port, it's stored in a buffer array before returning to Wait state. If no data is received, it directly goes back to Wait State.

2.4.4. Exit State

 doi:10.20944/preprints202406.0345.v1

Closes the serial port if it's open and then exits the LabVIEW application, or quits immediately if the port is closed.

In normal operation with the serial port open and actively receiving data, the state machine oscillates between Wait and GetData State, which allows for continuous data handling while promptly responding to user inputs.

2.5. Data Decoding

When buffer array updates, its content is matched against a predefined regular expression in LabVIEW. Upon a successful match, the segment is extracted with all preceding content is discarded and remainder is preserved for next matching. Ideally, when the microcontroller and host computer systems are functioning harmoniously, there should be no preceding content requiring deletion upon a successful match, ensuring efficient processing and presentation of impact data within the three-dimensional model.

2.6. Error Data Handling

A counter is working when superfluous data preceding the valid regex match appear. Then, the serial port is automatedly closed and subsequently reopened. This mechanism is validated to end the incorrect data frame alignment issues, which ensures the stable system operation.

2.7. Three-Dimensional Model Visualization Post-Data Decoding

A Sensor Mapping component is employed to visualize decoded sensor data on a three-dimensional human model. Sensors are attached on the corresponding locations on its surface, with the decoded data paired with its respective position on the model. Additionally, the model enables users to drag and rotate the model freely to view the impacted areas and magnitudes from any angle. The interactive ensures immediate understanding and assessment of the wearer's condition during hazardous situations.

A color gradient is assigned to represent sensor outputs. The output voltage is 1.65 V without deformation, which is defined to a value of 7 (depicted as green in the upper computer). Other colors and their corresponding values are showed in the color bar in the Figure 5.

The project prioritizes sensor placement in areas of high interest, focusing particularly on the heart region for enhanced location accuracy and sensitivity in measurements. Meanwhile, to mitigate the false cause by natural bending of limbs, the sensors number on the joint of knee and arm is reduced.

3. Results and Discussion

The sensor consistency is critical to ensure the location precision. The experiment setup employs a signal generator, a power amplifier, and a vibration platform to generate a fixed-frequency vibration. A standard signal generator is utilized to produce a 20 Hz sine wave, which enhances the load capacity after processed by the power amplifier. Thereafter, it drives the vibration platform to produce a sine wave vibration with the same frequency and fixed amplitude. By attaching mass to the end of the piezoelectric sheet, it deforms periodically when subjected to vibration.

The voltage response of sensor is directly observed by oscilloscope, and the corresponding acceleration is recorded using commercial accelerometer. The acceleration amplitude varies with the adjustment of signal generator voltage. by changing the output signal voltage. Data is recorded from multiple sensors under the same acceleration condition for comparison, with the results shown in Figure 4c. When subjected to a maximum sinusoidal vibration acceleration of 7 m/s^2, the sensor output voltage amplitude is 23.7±3.3 V, exhibiting excellent consistency.

Preprints.org (www.preprints.org) | NOT PEER-REVIEWED | Posted: 6 June 2024 doi:10.20944/preprints202406.0345.v1

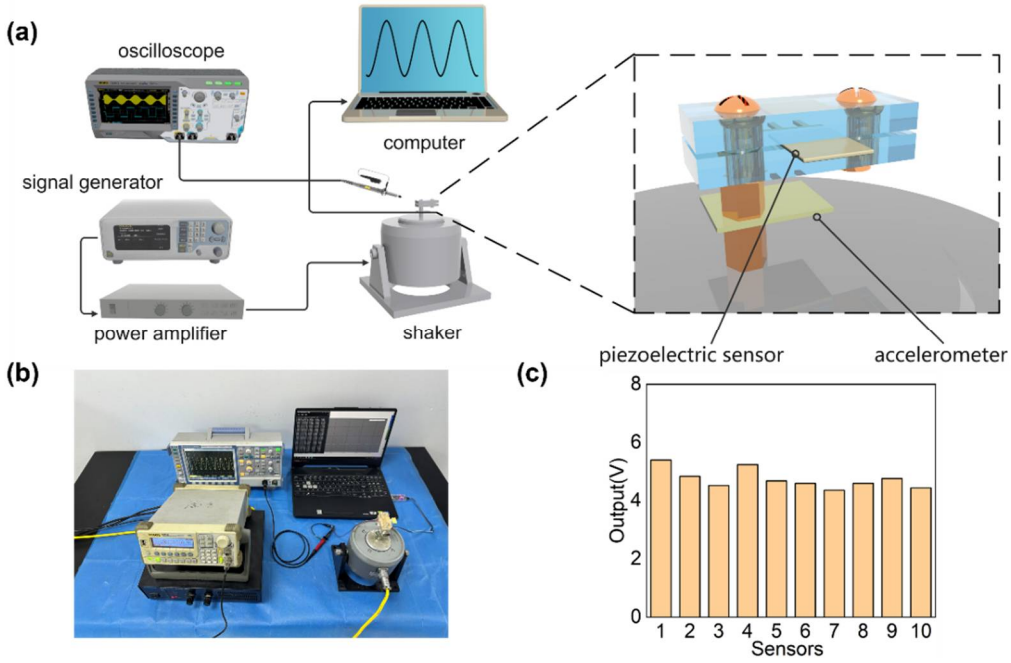

Figure 4. The measuring of the sensors'consistency. (a) Schematic diagram. (b)real object. (c)The sensor output under a acceleration amplitude of 7g.

Dress the fabricated protective suit onto a mannequin, and pair the Bluetooth module of the microcontroller system with the hardware Bluetooth module of the upper computer. When touching different parts of the mannequin, the upper computer system real-time displays the location and the magnitude of the impact on a 3D model. Compared to the commercial measuring equipment, the as-designed system achieves positional monitoring of different body parts, with the locations bias of 3.6±0.1 cm as shown in Figure 5.

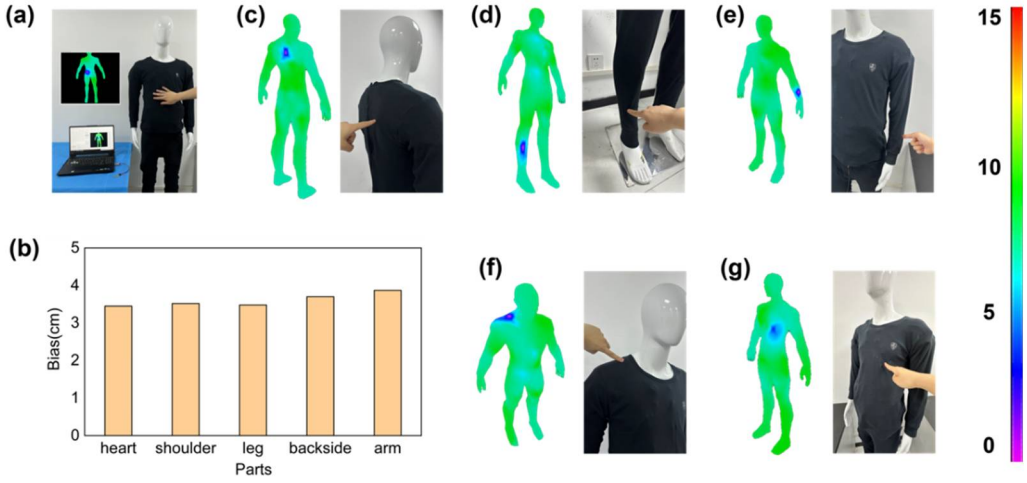

Figure 5. The result of the positioning precision. (a)Testing process. (b)The locations bias. (c)Backside. (d)Leg. (e)Limb. (f)Shoulder. (g)Heart.

Author Contributions: Conceptualization, C.L.; methodology, J.H.; software, J.H., Z.W.; validation, J.H., X.T. and X.W.; formal analysis, J.H, and F.L.; investigation, J.H. and X.W.; resources, X.T.; data curation, J.H. and Z.J.; writing—original draft preparation, J.H.; writing—review and editing, J.H. and C.L.; visualization, J.H.; supervision, C.L. and J.Y.; project administration, L.C., D.Y. and G.W.; funding acquisition, X.W. and L.D. All authors have read and agreed to the published version of the manuscript.

 doi:10.20944/preprints202406.0345.v1

Funding: This work was supported in part by the National Key R&D Program of China (No. 2022YFB3204800) and the Open Funding of Zhejiang Key Laboratory of Ecological and Environmental Big Data (No. EEBD-2022-02).

Institutional Review Board Statement: Not applicable.

Informed Consent Statement: Not applicable.

Data Availability Statement: The data used to support the findings of this study are available from the corresponding author upon request.

Conflicts of Interest: The authors declare no conflicts of interest.

References

1. Park, H.; Park, J.; Lin, S.-H.; Boorady, L.M. Assessment of Firefighters' needs for personal protective equipment. *Fashion and Textiles* **2014**, *1*, 1-13.
2. Jin, Q.; Tan, S.; Zhang, G.; Yang, Z.; Wen, Y.; Xiao, H.; Wu, X. Visible and Infrared Image Fusion of Forest Fire Scenes Based on Generative Adversarial Networks with Multi-Classification and Multi-Level Constraints. *Forests* **2023**, *14*, 1952.
3. Raimundo, A.M.; Figueiredo, A.R. Personal protective clothing and safety of firefighters near a high intensity fire front. *Fire Safety Journal* **2009**, *44*, 514-521.
4. Monea, B.F.; Ionete, E.I.; Spiridon, S.I.; Ion-Ebrasu, D.; Petre, E. Carbon nanotubes and carbon nanotube structures used for temperature measurement. *Sensors* **2019**, *19*, 2464.
5. Kane, C.; Mele, E.; Lee, R.; Fischer, J.; Petit, P.; Dai, H.; Thess, A.; Smalley, R.; Verschueren, A.; Tans, S. Temperature-dependent resistivity of single-wall carbon nanotubes. *Europhysics Letters* **1998**, *41*, 683.
6. Wang, Y.; Liu, J.; Zhao, Y.; Qin, Y.; Zhu, Z.; Yu, Z.; He, H. Temperature-triggered fire warning PEG@ wood powder/carbon nanotube/calcium alginate composite aerogel and the application for firefighting clothing. *Composites Part B: Engineering* **2022**, *247*, 110348.
7. Baksi, A.; Bhattacharjee, M.; Ghosh, S.; Bishnu, S.K.; Chakraborty, A. Internet of Things (IOT) based ambulance tracking system using GPS and GSM modules. In Proceedings of the 2020 4th International Conference on Electronics, Materials Engineering & Nano-Technology (IEMENTech), 2020. pp. 1-4,
8. Pettorru, G.; Pilloni, V.; Martalò, M. Trustworthy Localization in IoT Networks: A Survey of Localization Techniques, Threats, and Mitigation. *Sensors* **2024**, *24*, 2214.
9. Blecha, T.; Soukup, R.; Kaspar, P.; Hamacek, A.; Reboun, J. Smart firefighter protective suit-functional blocks and technologies. In Proceedings of the 2018 IEEE International Conference on Semiconductor Electronics (ICSE), 2018. pp. C4-C4,
10. Vallozzi, L.; Vandendriessche, W.; Rogier, H.; Hertleer, C.; Scarpello, M. Design of a protective garment GPS antenna. *Microwave and optical technology letters* **2009**, *51*, 1504-1508.
11. Li, Y.; Liu, C.; Zou, H.; Che, L.; Sun, P.; Yan, J.; Liu, W.; Xu, Z.; Yang, W.; Dong, L. Integrated wearable smart sensor system for real-time multi-parameter respiration health monitoring. *Cell Reports Physical Science* **2023**, *4*, 1-9.
12. Bruce-Low, S.; Cotterrell, D.; Jones, G. Effect of wearing personal protective clothing and self-contained breathing apparatus on heart rate, temperature and oxygen consumption during stepping exercise and live fire training exercises. *Ergonomics* **2007**, *50*, 80-98.
13. Tochihara, Y.; Lee, J.-Y.; Son, S.-Y. A review of test methods for evaluating mobility of firefighters wearing personal protective equipment. *Industrial health* **2022**, *60*, 106-120.
14. Liu, C.; Wang, Y.; Zhang, N.; Yang, X.; Wang, Z.; Zhao, L.; Yang, W.; Dong, L.; Che, L.; Wang, G. A self-powered and high sensitivity acceleration sensor with VQa model based on triboelectric nanogenerators (TENGs). *Nano Energy* **2020**, *67*, 104228.
15. Liu, C.; Fang, L.; Zou, H.; Wang, Y.; Chi, J.; Che, L.; Zhou, X.; Wang, Z.; Wang, T.; Dong, L. Theoretical investigation and experimental verification of the self-powered acceleration sensor based on triboelectric nanogenerators (TENGs). *Extreme Mechanics Letters* **2021**, *42*, 101021.
16. Kester, W. Which ADC architecture is right for your application. In Proceedings of the EDA Tech Forum, 2005. pp. 22-25,
17. Dan, S.; Yano, Y.; Wang, J. Batteryless BLE Module with a Piezoelectric Element Mounted on a Shoe Sole. *Sensors* **2024**, *24*, 2829.
18. Decharat, A.; Wagle, S.; Jacobsen, S.; Melandsø, F. Using Silver Nano-Particle Ink in Electrode Fabrication of High Frequency Copolymer Ultrasonic Transducers: Modeling and Experimental Investigation. *Sensors* **2015**, *15*, 9210-9227.
19. Gandelli, A.; Ottoboni, R. Charge amplifiers for piezoelectric sensors. In Proceedings of the 1993 IEEE Instrumentation and Measurement Technology Conference, 1993. pp. 465-468,

 doi:10.20944/preprints202406.0345.v1

20. Han, S.-J.; Jenkins, K.A.; Valdes Garcia, A.; Franklin, A.D.; Bol, A.A.; Haensch, W. High-frequency graphene voltage amplifier. *Nano letters* **2011**, *11*, 3690-3693.
21. Qiu, Y.; Shi, L.; Chen, L.; Yu, Y.; Yu, G.; Zhu, M.; Zhou, H. A Wide-Band Magnetoelectric Sensor Based on a Negative-Feedback Compensated Readout Circuit. *Sensors* **2024**, *24*, 423.
22. Shen, H.; Zhu, Z.; Lu, H.; Ju, H.; Huang, J.; Chen, Z. Development of a Sandwiched Piezoelectric Accelerometer for Low-Frequency and Wide-Band Seismic Exploration. *Sensors* **2023**, *23*, 9168.
23. Pinna, L.; Valle, M. Charge amplifier design methodology for PVDF-based tactile sensors. *Journal of Circuits, Systems and Computers* **2013**, *22*, 1350066.
24. Alnasser, E. A novel low output offset voltage charge amplifier for piezoelectric sensors. *IEEE Sensors Journal* **2020**, *20*, 5360-5367.
25. Kodosky, J. LabVIEW. *Proceedings of the ACM on Programming Languages* **2020**, *4*, 1-54.
26. Yang, B.; Guo, Y.; Wang, Z.D.; Gao, Y. Serial communication based on LabVIEW for the development of an ECG monitor. *Advanced Materials Research* **2013**, *734*, 3003-3006.
27. Lin, J.Q.; Xia, M.H.; Yang, W.L.; Leng, J. Design of Labview based equipment for measuring Thermally Stimulated Current. *Applied Mechanics and Materials* **2013**, *274*, 555-558.
28. Machacek, J.; Drapela, J. Control of serial port (RS-232) communication in LabVIEW. In Proceedings of the 2008 International Conference-Modern Technique and Technologies, 2008. pp. 36-40,
29. Win, M.T. Comparison Between Mealy and Moore State Models UsingSequence Detector with VHDL Coding Techniques. *International Journal of Advanced Research in Computer Engineering & Technology (IJARCET)* **2018**, *7*, 651-656.
30. Nedjah, N.; Mourelle, L.d.M. Mealy finite state machines: An evolutionary approach. *International Journal of Innovative Computing, Information and Control* **2006**, *2*, 789-806.